

# Ni-90 Superalloy Foam Processed by Space-Holder Technique: Microstructural and Mechanical Characterization

Gokhan Timac<sup>1</sup> and H.Ozkan Gulsoy<sup>2,\*</sup>

<sup>1</sup> Yalova University, Vocational School of Altinova, Machine and Metal Tech. Dep, 77100 Yalova, Turkey

<sup>2</sup> Marmara University, Technology Faculty, Metallurgy and Materials Eng. Dep., 34722 Istanbul, Turkey

\*Corresponding author, e-mail address: [ogulsoy@marmara.edu.tr](mailto:ogulsoy@marmara.edu.tr)

Received 7 July 2020; accepted 16 September 2020; published online 22 September 2020

## ABSTRACT

In this study, spherical and between 1400 to 1800  $\mu\text{m}$  carbamide particles coated with Ni-90 superalloys powder were used to produce foam by space-holder technique. Foams with porosity between 60%, 70% and 80 vol.% after mixing and compaction the space-holder particles were extracted using hot water leaching over a range of temperatures. The porous green parts were thermally debound to remove the paraffin wax under a pure argon atmosphere then sintered at high vacuum and subsequently heat treatment were performed. The effects of the volume fraction of space-holder particles on density and porosity were investigated. Microstructures were captured using optical and scanning electron microscopy. Also, compression tests were conducted on the sintered, heat treated samples.

## 1. INTRODUCTION

Traditionally, production of superalloy components begins with the fabrication of large ingots, and these ingots are used in three major production methods to obtain final products. One of these methods are remelting and producing superalloy powders [1]. Rapid solidification associated with powder metallurgy products provides homogeneous microstructures, fine grain structure and enhanced properties. Ni-based superalloys are an unusual group of metallic materials, showing an extraordinary combination of high temperature strength, toughness, and surface stability in corrosive or oxidative environments [1]. Nimonic alloys are one class of Ni-based superalloys developed to give superior creep resistance and are commonly used in wrought form. Nimonic type alloys gain their superior high temperature properties basically from the precipitation of Ni-Al-Ti compounds within a Ni-Cr matrix [2]. These intermetallic precipitates ( $\gamma'$ ) have an ordered cubic L12 structure, and the chemical formulation of

these phases is  $\text{Ni}_3(\text{Al}, \text{Ti})$ . ( $\gamma'$ ) phase is aluminium rich in most Ni-based superalloys and Ti rich in most Ni-Fe based superalloys [3, 4]. Ni-90 is designed to initially gain high-temperature strength by solid solution hardening brought about by Ni-Cr-Co base alloy strengthened by additions of Ti and Al [2, 3]. However, Ni-90 was designed to gain strength using solid solution initially. It has been developed as an ageing-hardenable creep resisting alloy for service at temperatures up to 920 °C. Given such superior characteristics, they are very important materials for high-temperature applications such as aerospace and power generation industries [5]. Ni-90 superalloy has been developed as an alloy that can harden by precipitation and resist creep under high temperature service conditions. Heat treatment is applied to Ni-90 superalloy to improve its properties or to allow a chemical process to be completed [30]. In particular, the microstructure of Ni-90 superalloys is highly dependent on heat treatment. The selection of the heat treatment to be applied is made according to the desired properties such as

hardness, resistance to breakage and corrosion. [31]. One of the Ni-based superalloys, which has been most successfully applied in the engineering applications, is Ni-90 alloy [6]. Ni-90 superalloy with proper development of the strength to weight ratio could be an alternative to other superalloys and foam materials [7, 8].

Metallic foam materials with controlled porosity are widely used in filtration, wicks, heat pipes, sound attenuation abradable seals, and flow control devices. Even lower densities are being promoted for energy absorption and applications requiring tailored mechanical, thermal, acoustic, and conduction properties [9, 10]. Metallic or ceramic foam materials (open-cell and close-cell) with a volume fraction of pores in the range of 5–80 % can be produced by different techniques (casting, sputter deposition, liquid-state processes – GASAR, and powder metallurgy) [9, 10].

Pore former and powder metallurgy (PM) with space-holder techniques have previously been demonstrated in the fabrication of other metallic and ceramic parts as well as stainless steel and low strength steels [13, 22]. With proper selection of the sintering cycle, the small particles will bond but the large intentional pores will remain. Thus, the process is composed of five sequential steps; (1) mixing of the powder, polymeric molding binder and space-holder particles, (2) compacting or shaping the mixture, for example by axial compression, (3) removing the binder phase and dissolving the space-holder particles without damaging the particle structure usually by a thermal step, (4) sintering the structure to induce strong particle bonding without densification of the pores remaining from the space-holder particles [8] and (5) heat treatment and aging process in sintered parts under suitable thermal cycle conditions. In the space-holder technique, the initial size and content of the space-holder particles provide the key control over the porosity, pore size, and pore connectivity [11, 12]. Several pore forming agents have been used in the past, including ice, salt, polymers, and volatile compounds such as camphor and ammonium bicarbonate ( $(\text{NH}_4)\text{HCO}_3$ ) [13, 14]. These have been combined with several metallic powders including aluminum, titanium, stainless steel, and Ni-based superalloys. Both carbamide ( $(\text{NH}_2)_2\text{CO}$  also known as urea) and ammonium bicarbonate

have been used with thermal extraction by heating below 180 °C; however, there are negative factors from the vapor release from these pore-forming parts [8, 11, 13].

In this work, porous Ni-90 superalloy was produced by the use of a water-soluble space-holder material to sintering. Spherical and specified dimensions carbamide particles were used as the space-holder material. Foams with porosity between 60, 70 and 80 % after mixing and compaction the space holder particles were extracted using hot water leaching over a range of temperatures. The porous green parts were thermally debound to remove the paraffin wax under a pure argon atmosphere then sintered at high vacuum and subsequently heat treatment and aging were performed. The effect of the volume fraction of space-holder particles on density and porosity of the sintered samples was investigated. Microstructures were captured using optical microscopy (OM) and scanning electron microscopy (SEM). Pore size was quantified using image analysis software integral to the SEM. Also, compression tests were conducted on the sintered, heat treatment and aging samples.

## 2. EXPERIMENTAL PROCEDURE

A schematic illustration of the production process is given in Fig. 1. The binder ingredient for green strength was paraffin wax with a melting range from 123 to 125 °C. It was used at 2 wt.% based on the Ni-90 superalloy mass. While preparing the mixture, Ni-90 superalloy powders and binder components in defined proportions calculated in the recipe were adjusted with a precise balance in determined amounts. Initially, the Ni-90 superalloy powders and paraffin wax were mixed using a double-cone mixer heated to 100 °C to melt the wax. Then carbamide particles is added to the mixture and mixing is done for 30 min was continued. The Ni-90 and carbamide particle ratios were adjusted to give 60, 70 and 80 vol % carbamide particles and paraffin wax in the samples.

Ni-90 superalloy powder used in this study was supplied by Sandvik Osprey Co. and it was produced by high pressure inert gas atomisation. The powder chemical properties were in Table 1. Particle size distributions were determined on

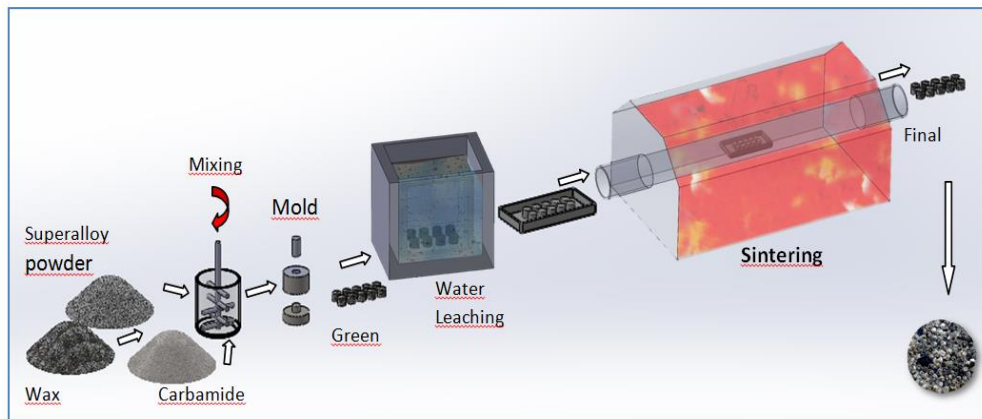


Figure 1. Processing steps of production of porous Ni-90 superalloy samples

Table 1. Chemical composition of Ni-90 superalloy powder

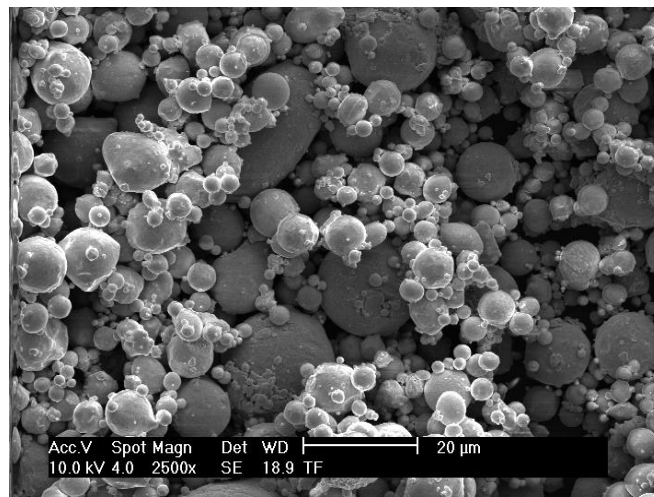
	wt. %								
Material	Ni	Cr	Co	Fe	Al	Ti	C	Si	Mn
Ni-90	57.38	19.50	17.3	0.68	1.02	2.40	0.082	0.94	0.69

Table 2. Physical characteristics of Ni-90 superalloy powder

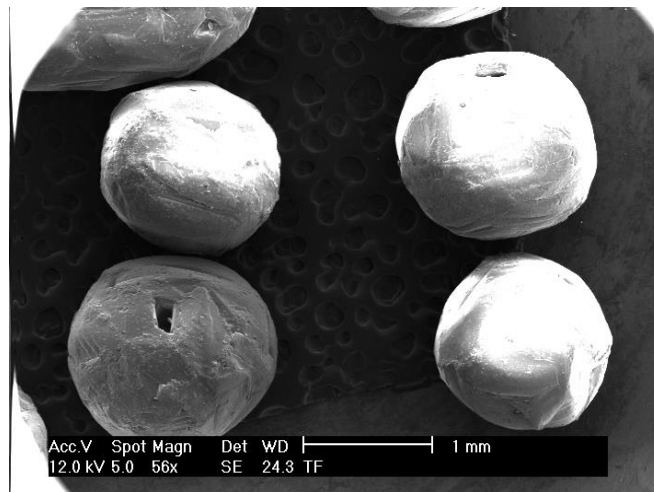
Item	Ni-90
Vendor	Sandvik Osprey Co.
Shape	Spherical
Tap Density, g/cm <sup>3</sup>	5.0
Theoretical density, g/cm <sup>3</sup>	8.26
Particle size	
D <sub>10</sub>	4.1
D <sub>50</sub>	11.0
D <sub>90</sub>	24.7

Malvern Master sizer equipment and are shown in Table 2. These indicate that the distribution of particle sizes is suitable for superalloy foam metal with powder metallurgy. The cumulative size distribution at the D<sub>10</sub>, D<sub>50</sub>, and D<sub>90</sub> percent points corresponds to particle sizes of D<sub>10</sub> : 4.1 μm, D<sub>50</sub> : 11.0 μm, and D<sub>90</sub> : 24.7 μm. Carbamide particles were used as space-holder. Carbamide density of 1.34 g/cm<sup>3</sup>, melting temperature of 133 °C, and

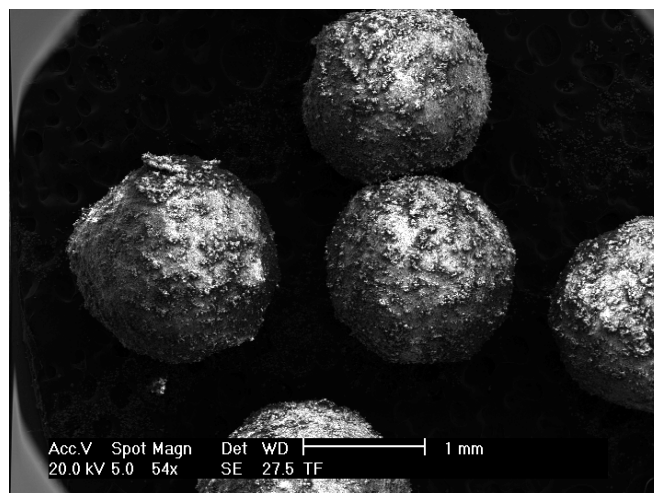
solubility in water at 20 °C of more than 1000 g/L. It was prepared as an irregular particle in a size range from 1400 to 1800 μm. The morphology of the powder and carbamide particle observed using SEM, is given in Fig. 2. The gas atomised Ni-90 superalloy powder and carbamide particle are spherical in shape. The SEM image of the coated carbamide particles with Ni-90 powder is given in Fig. 2.



(a)



(b)



(c)

Figure 2. SEM of (a) Ni-90 superalloy powder, (b) carbamide particles and (c) coated carbamide particles with Ni-90 superalloy powder

powders was performed in a Turbula mixer for 1 h. The mixtures were compacted at 100 MPa into cylinders with a diameter of 19 mm and height of 20 mm. The green samples which foams with porosity between 60, 70 and 80 % were held at 30 and 40 °C for times ranging from 1 to 6 h in distilled water for extracted using hot water leaching of carbamide particles. The paraffin wax was thermally removed as a part of the sintering cycle, which consisted of heating step-by-step at 1 °C/min to 600 °C with a 6 h hold, followed by heating at 5 °C/min to 900 °C for 1 h in high purity argon to pre-sinter samples. This was performed subsequent final sintering relied on a heating rate of 10 °C min<sup>-1</sup> to 1300 °C for 1 h under vacuum (10<sup>-3</sup> Pa). In this study, standards and Precision Castparts Corp. (Special Metals), the most suitable temperature and time for the aging and heat treatment of Ni-90 materials have been determined. The sintered samples were solution treated at 1080 °C for an hour as specified in the literature for alloy Ni-90 [15] and then cooled down in the water. The solution treated samples were aged at 705 °C for 16 h.

The density was calculated by dividing the mass of the compact by its volume, which was calculated from physical dimensions. Samples were mounted in epoxy and polished as standard metallographic procedures. Microstructures were obtained via OM (Olympus BX50) and SEM (FEI-Srion) after etching. Compression tests were performed at a crosshead speed of 1 mm/min. (Instron-8802

universal materials testing system). At least three specimens were tested under the same conditions to assess repeatability, and average values were used. After, the effect of the aging treatment was followed by hardness and X-ray diffraction (XRD) measurements. XRD analyses of the starting powder and the sintered and aged parts were performed out on a LabX- XRD 6100 device using Cu X-ray tube ( $\lambda=1.5405$ ) and with a 0.02/0.4 s. scanning step. Microhardness measurements of the sintered materials were performed on the HV<sub>0,2</sub> scale (Shimadzu).

### 3. RESULTS AND DISCUSSION

Ni-90 superalloy samples with porosity ranging between 60, 70, and 80 % were successfully produced temperature (slightly low for this material and particle size), the sintered density was 8.26 g/cm<sup>3</sup> (97% relative density). Sintered densities of 3.3 and 2.5 g/cm<sup>3</sup> (39,9% and 30,2% relative density) were obtained with 60 and 80 % carbamide particles additions, respectively. Fig. 3. shows the sintered and heat treated samples having 60, 70, and 80 % porosity. OM micrographs of the cell wall of foam are also shown. In all samples, the morphology of the pores was similar to that of the carbamide powder particles. The foams were observed to contain mainly two types of pores: macropores obtained as a result of carbamide space-holder and micropores on cell-

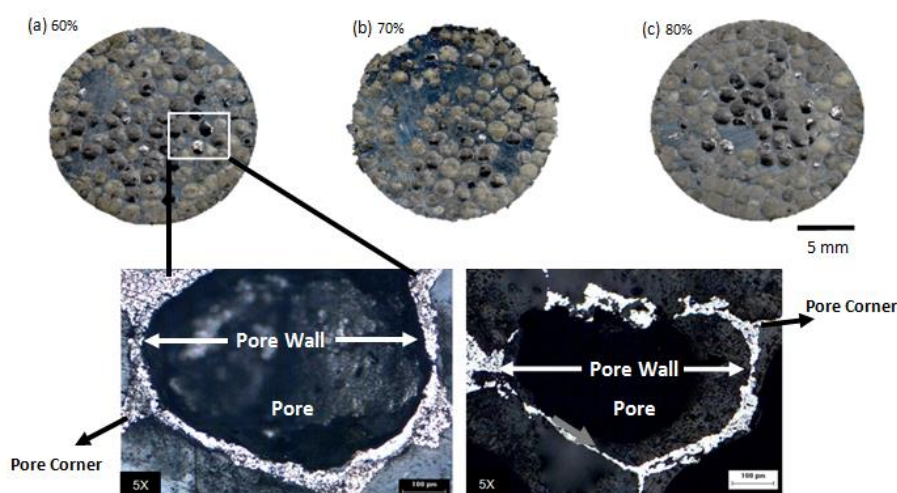
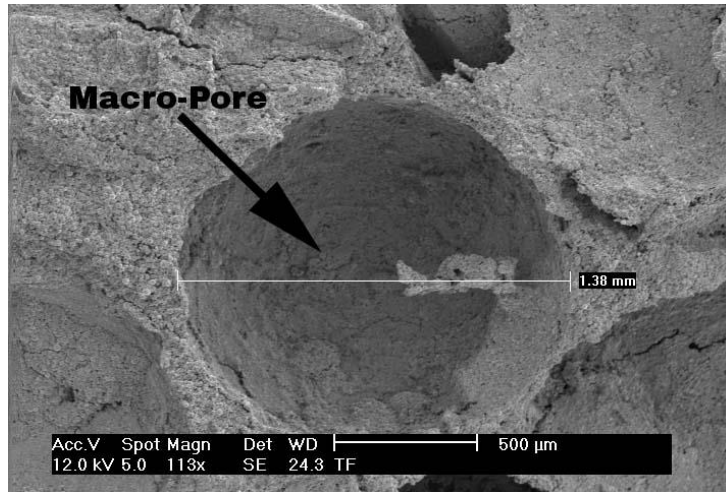
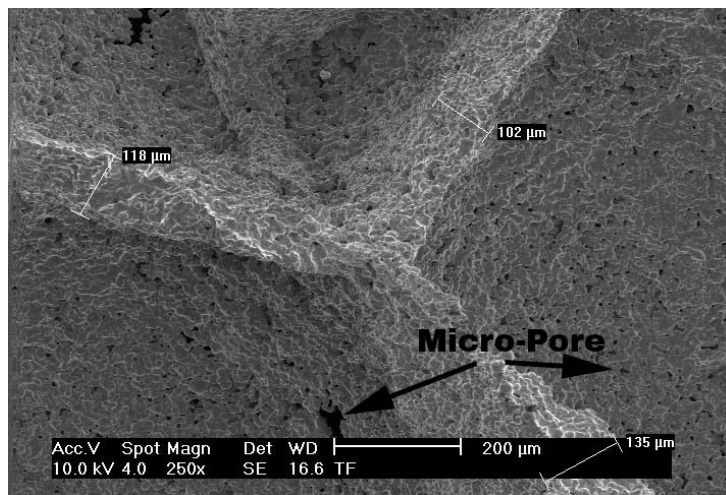


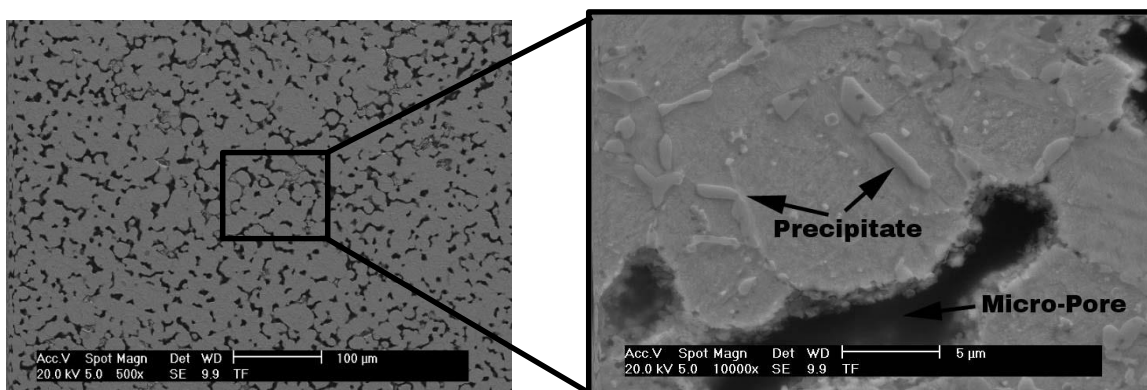
Figure 3. Macroscopic morphology of sintered Ni-90 superalloy samples from surface (a) sintered and aged for 60 vol. % (b) sintered and aged for 70 vol. % (c) sintered and aged for 80 vol. %



(a)



(b)



(c)

Figure 4. SEM micrographs of Ni-90 superalloy foam for 80 %, (a) heat treatment macro-pore, (b) aged micro-pore and (c) aged microstructure samples

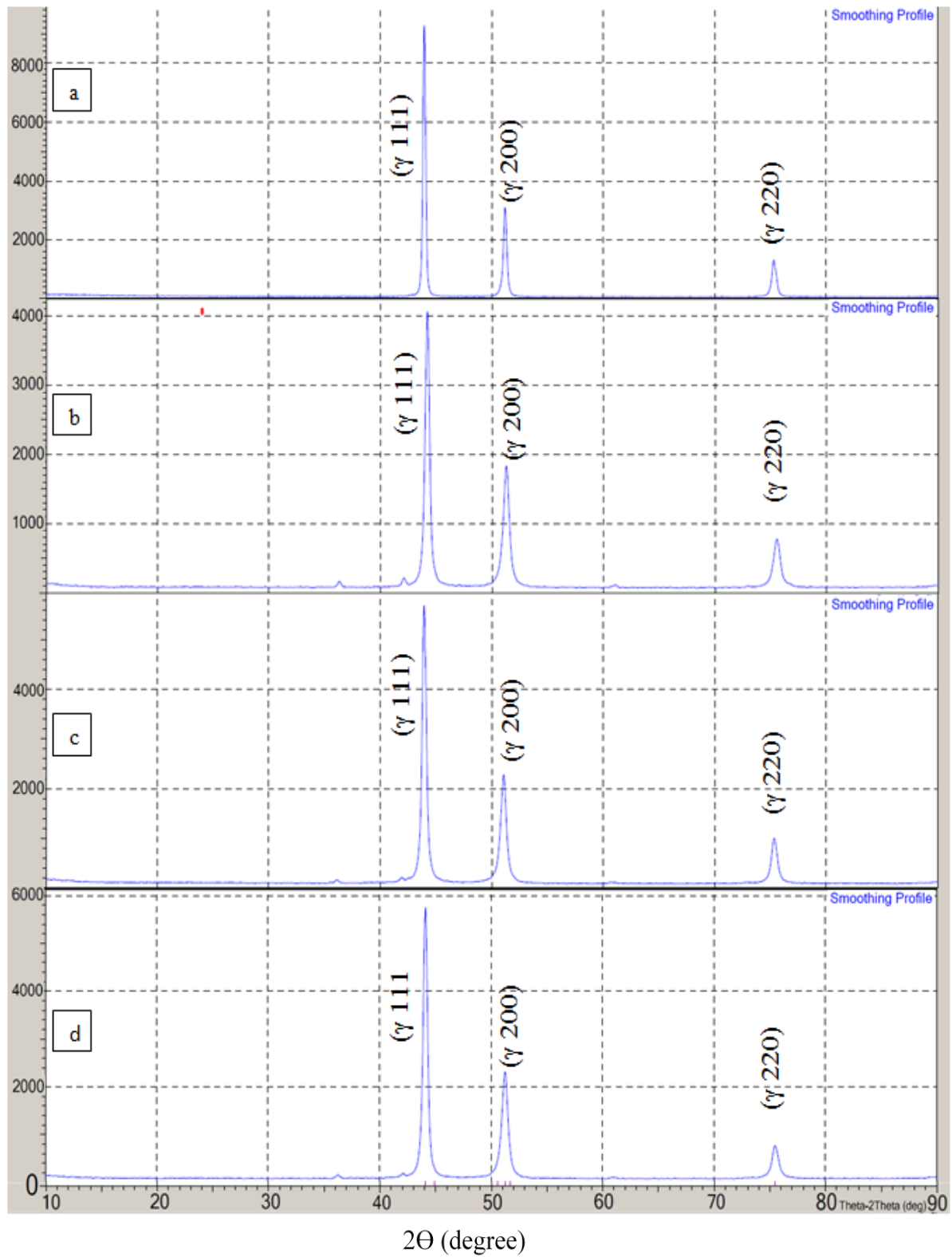


Figure 5. XRD diffraction patterns of (a) Ni-90 superalloy powder, (b) sintered, (c) solutioned and (d) aged samples

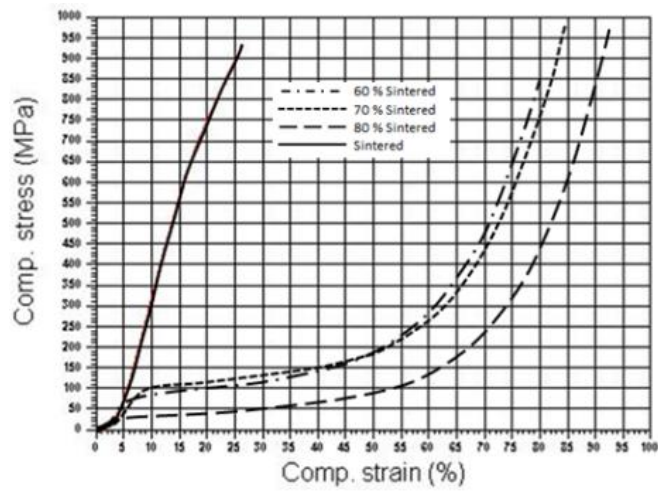
Ni-90 superalloy foam. By adjusting some space-holder particles, the porosity of the resulting Ni-90 foam can be altered. Macropores become directly connected above a porosity of 60 %, which may vary with the size of the space-holder particles and the powders constituting the cell walls [12, 16].

Fig. 4a shows the structure of a typical cell and the cell walls of Ni-90 superalloy foam produced by space-holder technique, which has a carbamide of 80 vol.%. The interconnecting cell channels are also clearly shown. Fig. 4b shows the bonding region between Ni-90 particles in the sample, indicating that strong bonds have formed between the particles. As can be seen in Fig. 4b, the microporosities existed in the sample. The microporosity in the sintered sample should be kept as low as possible if a high-strength porous metal solid were desired. SEM analysis was performed on heat-treated Ni-90 foams, as shown in Figure 4c. The basic phase that provides an increase in strength in most Ni-based superalloy which can be hardened by precipitation is  $\gamma'$  phase. Precipitation of the  $\gamma'$  phase in the matrix containing high Ni results in a significant increase in hardness and strength. The reason for this increase is thought to be the formation of  $\gamma'$  [Ni<sub>3</sub>(Al, Ti)] intermetallic precipitate and the smaller volume of  $\gamma'$  phase formed and homogeneous distribution for the whole structure during the aging time by heat treatment. This unique intermetallic phase is FCC-like, similar to the gamma matrix, and the lattice constant exhibits 1% or less incompatibility with the gamma matrix [17]. The  $\gamma'$  phase precipitation in the supersaturated matrix provides a significant increase in strength. Since the strength of the material will increase with the amount of  $\gamma'$  phase it contains, the volume ratio of the collapsed  $\gamma'$  phase is also important. The amount of  $\gamma'$  phase formed depends on the content of the hardening alloy element. These elements are strong  $\gamma'$  forming Al, Ti, Nb and Ta elements [17].

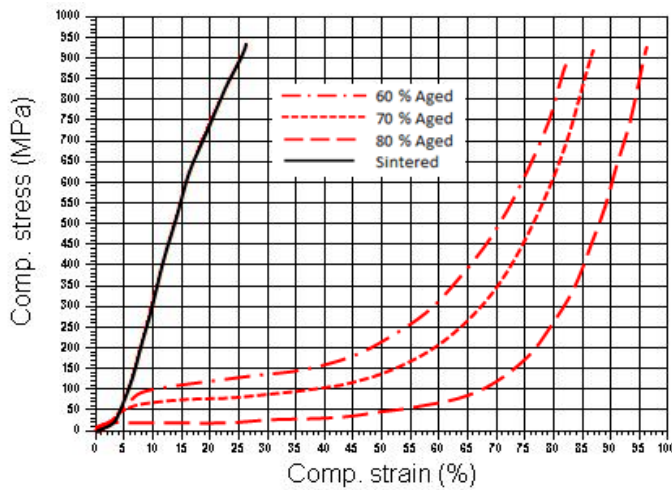
In order to understand whether there is phase change in microstructure due to sintering, cavity forming, heat treatment and aging processes the XRD analysis was performed. XRD analysis was performed on the following samples; prealloyed Ni-90 starting powder, sintered Ni-90 foam metal samples with 60-70-80 % porosity, Ni-90 sample sintered without porosity, heat treated Ni-90 foam metal samples with 60-70-80 % porosity and aged

Ni-90 foam metal samples with 60-70-80 % porosity. As a result of the XRD analysis, it was observed that the patterns obtained from all samples were almost the same. Some of their diffraction patterns are shown in Fig. 5. Carbide and  $\gamma'$  phase precipitates should be formed in the microstructure since the samples are left for cooling at 1000 °C/min without removing the tube from the furnace after sintering is performed for 1 hour at 1300 °C. However, the carbides (which are thought to be formed) and the intermetallic precipitates (which bring out the strengthening properties) are too small to be captured by XRD analysis. Carbides and especially intermetallic precipitates, which are the purpose of the aging treatment, cannot be detected by XRD analysis due to their low concentrations. However, it was indicated that the changes observed in the XRD patterns of the gamma matrix could be used to determine indirectly the presence of precipitates [18].

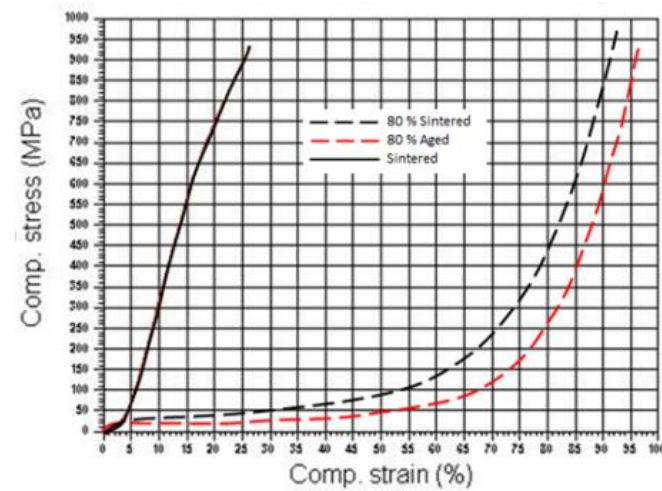
Fig. 6a. shows the compressive stress-strain curves of baseline and porous Ni-90 sintered samples with different fractions of carbamide. When the non-porous sample reaches 905 MPa stress (strain 25 %), the corresponding stress for carbamide-added samples at 60, 70, and 80 % are 52, 100.8, and 125.6 MPa, respectively. Fig. 6b. shows the compressive stress-strain curves of baseline and porous Ni-90 sintered and aged samples with different fractions of carbamide. When the non-porous sample reaches 905 MPa stress (strain 25%), the corresponding stress values for carbamide added samples at 60, 70, and 80 % are 24, 89.2, and 122.5 MPa, respectively. Fig. 6. shows a common stress–strain behavior characterized by three distinct regions (i.e., stress rising linearly with strain at low stresses (elastic deformation), followed by a strong plastic yielding for strains, and then a progressive densification regime where the cell walls come in contact one with another, causing an abrupt rise in the flow stress [7, 9, 10, 16, 19-22]. Once the cell edges collapse at the yield point, the collapsed edges have little ability to bear the load and bend easily. The deformation mode, resulting from the repeatable failure of the pore layers, gives rise to the uneven character of the stress–strain curve. The plateau region of the foam material subjected to the compression force is associated with the



(a)



(b)



(c)

Figure 6. Compressive stress- strain curves of porous Ni-90 superalloy foam samples with 60 – 80 % carbamide, (a) sintered samples (b) sintered and aged samples (c) sintered and aged for 80 vol. %

where the stress is constant, metallic porous materials have the ability to absorb energy without exceeding a certain stress limit [32, 33]. At the end of the plateau region, stress starts to increase since the pores have flattened and the material attains bulk-like properties. The plateau region has vital importance for the applications requiring energy absorption capability. Compression tests of the porous samples showed that the compressive strength values decreased and length of the plateau region increased with increasing porosity [9, 19, 23–27]. Fig. 6c. shows a comparison of sintered and aged samples for 80 % porosity. When compared the sintered and aged samples, strain values of the aged samples are higher than those of sintered samples. Depending on the aging process, elongation of the samples was developed. Since the carbamide particles are contained in the structure between 60,70 and 80% by volume and emerge as a void at the end of the process, the sintered density decreased. This increased the tension of porous samples. The strength of the samples increased as the porosity decreased.

## 5. CONCLUSION

In this study, defined sizes of spherical carbamide particles coated with Ni-90 superalloys powder were used to produce foam in powder metallurgy using the space-holder technique. Then sintered at high vacuum and subsequently heat treatment and aging were performed. Experimental results show that a carbamide pore former, nearly 100-fold larger than the Ni-90 superalloy particles, provides a means to retain large pores in the sintered part. By extraction of the carbamide by water leaching after compaction, medium density Ni-90 superalloy foams are realized by a traditional powder metallurgy route. The green compact had sufficient strength for handling after water leaching at sintering stages. Metallographic studies revealed a relatively uniform distribution in the sintered structure when the two-dimensional visual structures of the top, bottom and cut samples of samples with 60, 70 and 80% porosity were examined. Large numbers of micropores formed in the cell-walls due to insufficient solid-state sintering. No distortion or other visible reduction in part quality or surface finish was observed at 1300 °C for 1h under vacuum and for aged 705 °C. When

the morphology images are examined, it is seen that the pores are mostly between the grains and there are almost no pores trapped in the grain. It has been observed that the grain size of the material has slightly increased with the sintering process. By comparing the physical and mechanical properties of the samples with the homogeneous porous structure, sintered density decreased, porosity increase with a fraction of space-holder particles increment was observed. Compression tests have shown that heat treatment increases the strength values of the Ni- 90 alloy. As a result of XRD analysis, no pike other than gamma matrix peaks was found in the patterns of both the starting powder, the pore-free sintered and the aged sample. It is thought that after sintering and aging, carbide and  $\gamma$  'phase precipitates should be formed in the microstructure. However, it is thought that the carbides thought to be formed and especially the intermetallic precipitates, which are the purpose of the aging process, are in such small quantities that cannot be detected by XRD analysis. Comparing the XRD patterns, the decrease in the intensity of the gamma matrix peaks in the sintered sample compared to the starting powder indicates that after the sintering process, a large amount of precipitate phase was formed in the material.

## ACKNOWLEDGEMENTS

This study was supported by the Scientific Research Projects Coordination Unit of Marmara University, Project number FEN-C-DRP-090512-0172. The authors are grateful to Sandvik Osprey Co. for their financial support and the provision of laboratory facilities.

## REFERENCES

- [1] T.M. Pollock, S. Tin, *J. Propul. Power* **22**, 361–374 (2006).
- [2] W. Betteridge, (1959) The Nimonic alloys, Edward Arnold Ltd. London.
- [3] E.W. Ross, C.T. Sims, (1987) Superalloys-II., John Wiley & Sons. New York.
- [4] E.F. Bradley, (1988) Superalloys: a technical guide, ASM International. Metals Park, OH.
- [5] S.L. Semiatin, K.E. McClary, A. D. Rollett, C. G. Roberts, E. J. Payton, F. Zhang & T. P. Gabb, *Metall. Mater. Trans. A*, **43**, 1649-1660 (2012).
- [6] M.J. Cieslak, (1991) Proceedings of the International Symposium on the Metallurgy and Applications of

- Superalloys 90, 625 and Various Derivatives. TMS, USA.
- [7] J. Kovacic, J. Jerz, N. Minarikova, L. Marsavina, E. Linul, *Frattura ed Integrità Strutturale* **36**, 5563 (2016).
- [8] H.O. Gulsoy, R.M. German, *Pow. Metall.* **51**, 350-353 (2008).
- [9] Eds. M.F. Ashby, A.G. Evans, N.A. Fleck, L.J. Gibson, J.W. Hutchinson, H.N.G. Wadley, (2000) *Metal Foams: A*, Elsevier Inc.
- [10] A.E. Simone, L.J. Gibson, *Acta Mater.* **44**, 1437-1450 (1996).
- [11] B. Jiang, N.Q. Zhao, C.S. Shi, J.J. Li, *Scripta Mater.* **53**, 781-785, (2005).
- [12] D.J. Sypeck, P.A. Parrish, H.N.G. Hayden, (1998) Materials Research Society Symposium Proceedings. 205-219., MRS, USA.
- [13] Y.Y. Zhao, D.X. Sun, *Scripta Mater.* **44**, 105-110 (2001).
- [14] Martin Bram, Cornelia Stiller, Hans Peter Buchkremer, Detlev Stöver, Hartmut Baur, *Adv. Eng. Mater.* **2**, 196-199 (2000).
- [15] O. Ozgur, H.O. Gulsoy, R. Yilmaz, F. Findik, *J. Alloys and Comp.* **576**, 140-155 (2013).
- [16] N. Michailidis, F. Stergioudi, A. Tsouknidas, E. Pavlidou, *Mater. Sci. Eng. A*, **528**, 1662-1670 (2011).
- [17] G.L. Erickson, (2005) Polycrystalline Cast Superalloys. In *Asm Handbook: Properties And Selection: Irons, Steels, And High Performance Alloys*, 1:1532-1550, ASM, USA.
- [18] R.B. Li, M. Yao, W.C. Liu, X.C. He, *Script. Mater.* **46**, 635-638 (2002).
- [19] J. Banhart, *Prog. Mater. Sci.* **46**, 559-570 (2001).
- [20] J. Kovacic, F. Simancik, *Kovove Mater.* **42**, 79-90 (2004).
- [21] D.C. Dunand, *Adv. Eng. Mater.* **6**, 369-375 (2004).
- [22] H.I. Bakan, *Scripta Mater.* **55**, 203-208 (2006).
- [23] N. Bekoz, E. Oktay, *Mater. Process. Tech.* **212**, 2109-2116 (2012).
- [24] M. Kohl, T. Habijan, M. Bram, H.P. Buchkremer, D. Stover, M. Koller, *Adv. Eng. Mater.* **11**, 959-968 (2009).
- [25] A. Bansiddhi, D.C. Dunand, *Mater. Eng. and Perf.* **20**, 511-516 (2011).
- [26] I. Mutlu, E. Oktay, *Mater. Sci. Eng. C*, **33**, 1125-1131 (2013).
- [27] I. Mutlu, E. Oktay, *Mater. Des.* **44**, 274-282 (2013).
- [28] R.J. Mitchell, C.M.F. Rae, S. Tin, *Material Science And Technology* **21**, 125-132 (2005).
- [29] M. Sundararaman, *Mineral Processing and Extractive Metallurgy Review* **22**, 681-700 (2002).
- [30] Mj. Donachie, Sj. Donachie, (2002) Selection Of Superalloys For Design. In *Handbook Of Material Selection*, John Wiley & Sons, Inc. B, 10: 293-334.
- [31] M. Retima, S. Bouyegh, H. Chadli, Effect Of The Heat Treatment On The Microstructural Evolution Of The Nickel Based Superalloy. *Metalurgija-Mjom.* **17(2)**, 71-77 (2011).
- [32] Cs. Kadar, P. Kenesei, J. Lendvai, Zs. Rajkovits, Energy absorption properties of metal foams, *VI. évfolyam 1. szám*, **6**. (2005).
- [33] C.Wang, R. Li, Effect Of Double Aging Treatment On Structure In Inconel 718 Alloy, *Journal of Materials Science*, **39**, 2593 – 2595. (2004).